Revue Phys. Appl. **15** (1980) 277-283

FÉVRIER 1980, PAGE 277

Classification
Physics Abstracts
62.20F — 81.40C

Plastic deformation of CoO single crystals

J. Castaing, M. Spendel, J. Philibert

Laboratoire de Physique des Matériaux, C.N.R.S. Bellevue, 92190 Meudon, France

A. Dominguez Rodriguez and R. Marquez

Departamento de Optica, Facultad de Ciencias, Universidad, Sevilla, Espagne

(*Reçu le 27 juin 1979, révisé le 16 octobre 1979, accepté le 17 octobre 1979*)

Résumé. — Des essais de compression à vitesse constante ($\dot{\varepsilon} \sim 6 \times 10^{-5}\ s^{-1}$) ont été réalisés selon une direction $\langle 001 \rangle$ de monocristaux de CoO. La contrainte à la limite élastique et le taux de consolidation ont été déterminés entre 77 K et 1 400 K. Leurs valeurs sont très élevées par rapport à celles de composés similaires. La microdureté Vickers a été mesurée sur les faces { 100 }, { 110 } et { 111 } entre 0 °C et 40 °C, températures encadrant le point de Néel. La dureté de CoO est faible par comparaison avec les caractéristiques de déformation à vitesse constante ; elle montre une faible anomalie à la température de Néel.

Abstract. — Constant strain rate compressions along $\langle 001 \rangle$ have been performed on CoO single crystals ($\dot{\varepsilon} \sim 6 \times 10^{-5}\ s^{-1}$). Yield stresses and work hardening rates have been measured between 77 K and 1 400 K ; CoO is very strong when compared to similar compounds. Vickers indentations have been performed on { 100 }, { 110 } and { 111 } faces around the Néel temperature, i.e. between 0 °C and 40 °C. Hardness values are low if compared to constant strain rate deformation characteristics ; they show a minor anomaly at the Néel temperature.

1. **Introduction.** — Cobaltous oxide is one of the NaCl structure oxides of transition metals. The corresponding metals are used in many high temperature applications in oxidizing atmosphere ; the oxidation rate is diffusion controlled provided the oxide scale does not break. To avoid fracture, interfacial stresses must be relieved by plastic deformation. It is then of considerable interest to study mechanical properties of transition metal oxides.

Nickel oxide has received little attention [1], [2], [3], while cobaltous oxide CoO has been more extensively studied at high temperature ($T > 1\,000$ °C i.e. $T > 0.6\ T_M$) [3-9]. These two oxides appear to be similar with metal deficient nonstoichiometry, NaCl type crystal structure (lattice parameter 0.418 nm for NiO and 0.426 nm for CoO) and antiferromagnetic ordering at low temperature ($T_N = 525$ K for NiO and 290 K for CoO). It is then interesting to compare their mechanical properties which should show similarities also with other ionic compounds (LiF, NaCl, MgO).

However, CoO is a more complicated compound ; it is not stable in air below 900 °C where it oxidizes [10-11] giving a Co_3O_4 spinel phase (Fig. 1).

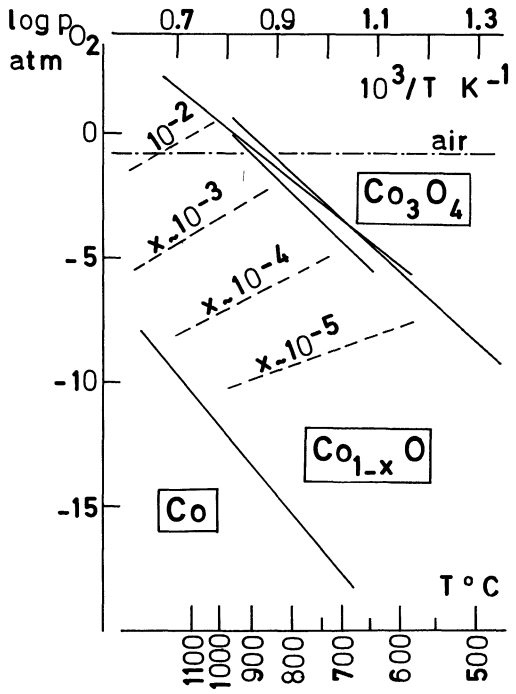

Fig. 1. — Stability relations of Co, CoO and Co_3O_4 as determined by various investigators [10], [11], [12], [15] (1 atm ≃ 10^5 Pa).

The use of quenched specimens allowed us to investigate the low temperature plastic behaviour of CoO single crystals provided the phase transformation does not occur.

The phase change kinetics from CoO to Co_3O_4 has not been studied on single crystals, but on polycrystals (grain size below 20 nm [14], specific surface of 0.3 m^2/g [13] and porosity between 25 % and 27 % [12]) which, probably, show much faster oxidation. Below 200 °C, no oxidation occurs; above this temperature, it takes several hours to yield a measurable amount of Co_3O_4. We can conclude that, at the time scale of our experiments (1 h), mechanical tests were performed, below 500 °C, on CoO single crystals without any layer of Co_3O_4. For sintered material, the oxidation rate in air is maximum at 800 °C and negligible above 900 °C and below 700 °C [12]; one hour at 800 °C gives a 4 % fraction of reaction from CoO to Co_3O_4 corresponding to a thickness of 20 μm on single crystals. Such layers should not influence the plastic properties of the bulk crystal.

After giving a few details on experimental techniques (crystal growth, specimen preparation, plastic deformation), we shall describe mechanical data i.e. yield stress, workhardening rate and microhardness value for various temperatures; finally, we shall discuss the origin of the great strength of CoO crystals.

2. **Experimental techniques.** — 2.1 SPECIMEN PREPARATION. — The single crystals employed in this study were grown by the zone melted technique in an arc image furnace [16]. The sintered rod which feeds the melt, was obtained from high purity CoO powder (Johnson Matthey; Si-7 ppM, Fe-2 ppM). The crystals were oriented using the back-reflection Laue X ray technique; they were cut along { 100 } faces, into compression specimens of approximately $2 \times 2 \times 5.5$ mm^3 ($\pm$ 0.1 mm) [17], before annealing in air at 1 200 °C for at least two days. The aims of this annealing are to (i) dissolve any Co_3O_4 precipitate (ii) obtain a standard reference state for as-grown dislocation structure (iii) ensure nonstoichiometry equilibrium, as CoO is known to be a metal deficient oxide with singly ionized metal vacancies above 950 °C [15].

The kinetics of processes (i) and (iii) is controlled by vacancy migration; the chemical diffusion coefficient $\tilde{D}$ can be computed from [28]. We obtain a value $\tilde{D} = 2.6 \times 10^{-6}$ cm^2/s at 1 200 °C and $\sqrt{\tilde{D}t} = 1$ mm for one hour and 4.7 mm for one day; at 950 °C, $\tilde{D} = 3.9 \times 10^{-7}$ cm^2/s and $\sqrt{\tilde{D}t} = 0.4$ mm for one hour and 1.8 mm for one day. These values indicate that the chosen annealing conditions allow to reach equilibrium and that, during the mechanical test time (1 h), the specimen does not change appreciably in the bulk below 950 °C.

The annealing conditions were within the CoO stability range (Fig. 1) and in order to avoid Co_3O_4 formation, the specimens were air quenched; however, a very thin oxide layer was revealed by the tarnishing of the surface.

For microhardness test, the crystals were cut along { 100 }, { 110 } and { 111 }. They were then annealed in air at 1 200 °C for 48 h and air quenched. After a mechanical polish, a chemical polish was performed using various conditions summarized in table I.

Table I. — *Chemical polishing of* CoO.

Face	Chemical etchant	Temperature	Polishing time
(100)	H_3PO_4	75 °C	10 min
(110)	HNO_3 (50 %) H_3PO_4 (50 %)	85 to 90 °C	5 to 7 min
(111)	H_3PO_4	80 °C	3 to 4.5 min

2.2 COMPRESSION TESTS. — The specimens were tested in compression along ⟨ 100 ⟩ in an Instron machine at a crosshead velocity of 20 μm/min ($\dot{\varepsilon} \sim 6 \times 10^{-5}$ s^{-1}). For high temperature tests, the equipment is the same as that used in [2]; most of the tests were performed in air and thermal equilibrium was reached within one hour. For low temperature tests (− 196 °C to 300 °C) a compression jig made of Inconel steel was used. Its design allows to immerse the specimen in a liquid held at the desired temperature : oil or water for intermediate temperatures, cooled aceton or liquid nitrogen for lower temperatures.

The stress and strain values plotted in the figures are engineering ones.

2.3 MICROHARDNESS MEASUREMENTS. — The microhardness was measured with a Vickers diamond using a Zeiss tester. Loads between 20 g and 100 g were applied giving the same hardness values. Throughout this study, we used a 50 g load applied during 30 s. This duration is not critical since for variations between a few seconds and a few minutes no significant change was observed in hardness values.

Temperature variations from 1 °C to 40 °C were obtained using a device built on this purpose. The specimen and thermocouple were glued on a brass piece through which water flowed at the desired temperature. The whole assembly was immersed in silicone oil which kept the Vickers diamond at the testing temperature. Measurements were made at increasing temperatures.

At room temperature, the hardness value was the same for tests performed either in air or in silicone oil.

3. **Results.** — 3.1 PLASTIC DEFORMATION IN COMPRESSION. — Stress-strain curves are shown in figure 2. Plastic deformation of more than 1 % could be

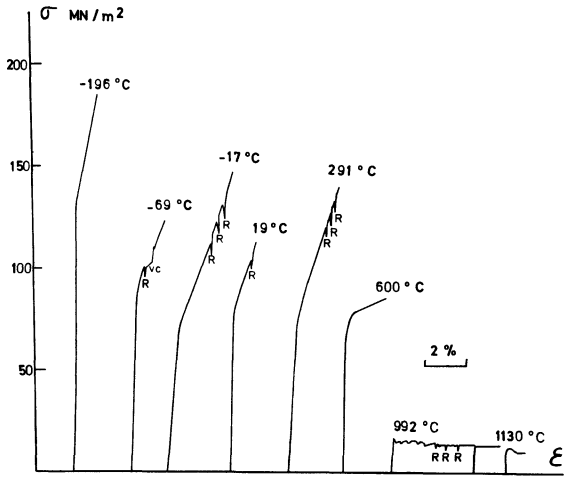

Fig. 2. — Engineering stress-strain curves for CoO single crystals from liquid nitrogen temperature to 1 130 °C. Tests above 600 °C were performed in air. Relaxations are indicated by R and one strain rate change by VC (1.5×10^{-5} s^{-1} and 6×10^{-5} s^{-1}).

observed at liquid nitrogen temperature where CoO shows a larger ductility than NiO [18]. At high temperature (~ 1 000 °C) unstable yielding appears, with stress drops of about 7 % followed by a slow increase of stress as deformation proceeds. This instability disappears after repeated relaxations and after unloading followed by immediate reloading.

Figure 3 shows the yield stress, the flow stress for 0.2 % strain and the work hardening rate for various temperatures. Above 900 °C, the drops of CoO strength is probably related to the phase transformation (Fig. 1). A few deformations have been performed straining the same specimen either with temperature changes between 1 000 °C and

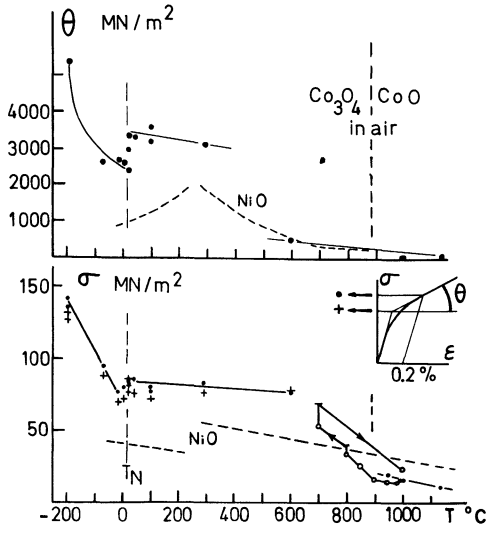

Fig. 3. — Variation with temperature of engineering yield stress, flow stress for 0.2 % strain and work-hardening rate ($\theta = d\sigma/d\varepsilon$). One sample was strained to 14 % between 1 000 °C and 700 °C in air ; vertical bars indicate hardening at fixed temperature (work-hardening or ageing). T_N is the Néel temperature. The curves for NiO after ref. [2] are also shown.

700 °C (Fig. 3), or with oxygen pressure changes between air and argon ($p_{O_2} \sim 10^{-6}$ atm) at about 775 °C (Fig. 4) ; in both cases, the specimen is brought in and out of the Co_3O_4 phase field along constant p_{O_2} or constant T lines (Fig. 1).

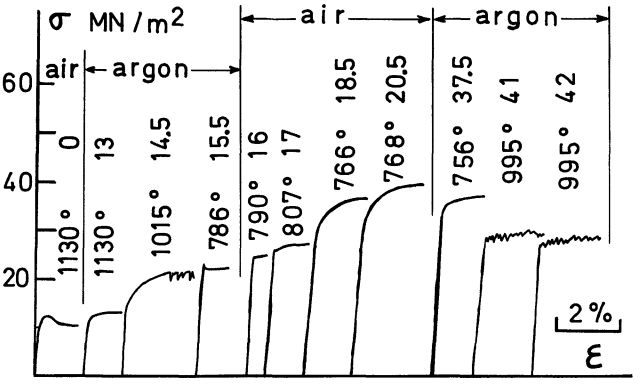

Fig. 4. — Stress-strain curves for the same CoO crystal deformed at various temperatures in air and argon. Temperatures are in degrees celsius. The time of the test is indicated in hours ; before the first test, the sample was annealed 22 h at 1 220 °C in air.

The results of the first kind of experiments are schematically reported on figure 3 where arrows show the thermal cycle. In the CoO phase field, plastic flow appears abruptly, after a yield drop for the first deformation (Fig. 2). On the contrary, the stress strain curves show a gradual change from elastic to plastic behaviour for experiments after a while in Co_3O_4 conditions. No yield drop appears after several hours ageing in air at 700 °C, but the crystal slowly hardens with time. The values of the flow-stress measured between 1 000 and 700 °C fits with both low and high temperature ones (Fig. 3).

The results of the second kind of experiments are shown in figure 4. The strength of CoO slightly increases with decreasing oxygen pressure at 1 130 °C in agreement with creep experiments [4]. The flow stress increases slightly when temperature decreases down to 786 °C i.e. in the stability conditions of CoO (Fig. 1) ; these flow stress values are relative to stable CoO ; so, they are nearly the same as those plotted in figure 3 above 900 °C, but they are much smaller at 786 °C. When the atmosphere is changed at a constant temperature of about 770 °C, CoO becomes harder in air (as it enters Co_3O_4 phase field, Fig. 1) and softer in argon.

Unstable yielding has not been observed for the first deformations, but it appeared suddenly after 1 % strain at 1 015 °C in argon. It was not observed for the first deformation back in the CoO phase field (756 °C and 838 °C argon), but appeared at 995 °C from the beginning of plastic deformation. This phenomenon seems related to tests performed close to 1 000 °C (Figs. 2 and 4).

3.2 MICROHARDNESS. — The variation of microhardness with temperature is shown in figure 5. The values for indentations on { 110 } and { 111 } are the same; they gradually decrease with increasing temperature. At the Néel temperature ($T \simeq 18$ °C [19]), the curve seems to show a minor anomaly; a much larger anomaly occurs for the { 100 } hardness values which, otherwise, are identical below 10 °C and above 25 °C.

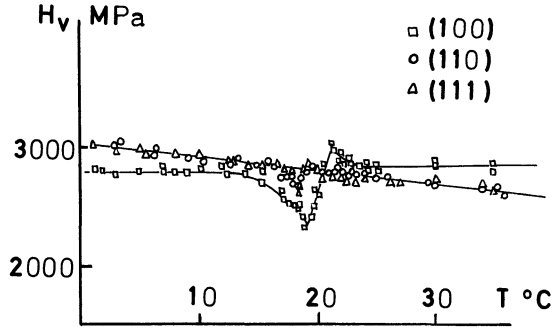

Fig. 5. — Variations with temperature of hardness value H_V for indentation on { 100 }, { 110 } and { 111 } faces. Each point is the average of 5 values (standard deviation : 50 mPa).

The same hardness tests have been performed on a less pure specimen (99.9 % instead of 99.995 %) which should be harder; however, { 110 } and { 111 } values are smaller of about 3 % and { 100 } values of 12.5 % at 1 °C. The shape of the curves are similar to that of figure 5, the anomaly at the Néel temperature appearing 2 °C below.

4. **Discussion.** — 4.1 LOW TEMPERATURE PLASTIC PROPERTIES. — The plastic behaviour of CoO appears similar to that of NaCl type compounds. Optical observations of slip lines showed the usual ⟨ 110 ⟩ { 1$\bar{1}$0 } slip system after room temperature deformation. Large ductility is obtained even at liquid nitrogen temperature (77 K); CoO is stronger than NiO below 900 °C and softer above this temperature (Fig. 3). Figure 6 shows the engineering yield stress normalized by the shear modulus μ *vs.* reduced temperature for several rocksalt structure crystals. The values of μ have been taken for CoO either as $\mu_1 = 1/2(C_{11} - C_{12})$ or as $\mu_2 = \sqrt{C_{44}\dfrac{C_{11} - C_{12}}{2}}$. It is not obvious if one must use μ_1 or μ_2; there is no difference for isotropic medium, i.e. above the Néel temperature for CoO ($A = 2\,C_{44}/(C_{11} - C_{12}) \sim 1.5$). Below the Néel temperature, CoO shows large elastic anisotropy ($A \sim 6$) leading to the two σ/μ curves (Fig. 6). We have used μ_1 and μ_2 values constant, except in the vicinity of the Néel temperature, with $\mu_1 \sim 0.15 \times 10^{11}$ Pa, $\mu_2 \sim 0.35 \times 10^{11}$ Pa below 273 K, and $\mu_1 \sim 0.58 \times 10^{11}$ Pa, $\mu_2 \sim 0.7 \times 10^{11}$ Pa above 298 K [20].

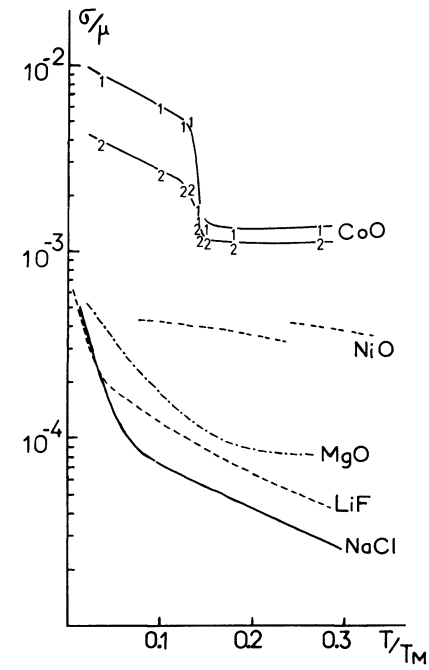

Fig. 6. — Variations with normalized temperature T/T_M of engineering yield stress-shear modulus ration σ/μ for various NaCl compounds. CoO : $T_M = 2\,075$ K; NiO : $T_M = 2\,235$ K. MgO : $T_M = 3\,098$ K; LiF : $T_M = 1\,113$ K; NaCl : $T_M = 1\,074$ K. For CoO points 1 represent σ/μ_1 and point 2 σ/μ_2.

The large increase of elastic constants at the Néel temperature inverts and magnifies, on figure 6, the small anomaly visible on the σ-T curve (Fig. 3).

Values of σ/μ for NiO have been plotted with σ from [2] and $\mu = 1.03 \times 10^{11}$ Pa below the Néel temperature (0.234 T_M) and $\mu = 1.35 \times 10^{11}$ Pa above it.

Figure 6 shows results for other extensively studied ionic compounds. For LiF, we plotted σ values [21] using constant $\mu = 0.41 \times 10^{11}$ Pa as for MgO [22] with $\mu = 1.25 \times 10^{11}$ Pa. For NaCl, plotted data use $\mu = 1/2(C_{11} - C_{12})$ depending on temperature [23].

CoO is the strongest material in figure 6; this suggest that the obstacles to dislocation motion are very strong in CoO below 0.3 T_M. For MgO, obstacles are impurities and the Fleisher theory accounts for the observations according to [22]; activation volumes V between 100 b^3 and 400 b^3 have been measured [24] where b is the dislocation Burgers vector.

In NaCl, the obstacles would be forest dislocations according to V between 400 b^3 and 1 500 b^3 [23]. Below 50 K the deformation rate of LiF seems to be controlled by a Peierls mechanism; activation analysis gives V values between 20 b^3 and 70 b^3 [21]. These three compounds show very similar behaviour on figure 6, although different obstacles to dislocation motion have been invoked. The σ/μ curve for CoO is different from that of other compounds; this suggests that a new rate controlling mechanism may be operative, perhaps related to the tetragonal deformation of the lattice which occurs below the Néel

temperature; this tetragonal deformation increases with decreasing temperature ($c/a = 0.988$ at about 100 K [26]). It leads to domain structure with boundaries very often in { 101 } plane [25].

We have measured the activation volume using stress relaxation and strain rate change techniques [2].

Below 0 °C, the activation volume of CoO, determined by stress relaxation, is between 80 b^3 and 200 b^3. It increases to values of 600 b^3 above 0 °C; the transition width is about 100 K, much larger than that for the magnetic transition [19], [20]. This suggests that the rate controlling mechanism for dislocation motion changes around the Néel temperature, a low temperature regime being replaced by a high temperature one. Further analysis of the activation process of plastic deformation is necessary to draw a firm conclusion; the results suggest that a lattice friction arises in the antiferromagnetic state. Above the Néel temperature, obstacles to dislocation motion could be point defects or forest dislocations.

The yield stresses of CoO are very large, so are the work hardening rates $\theta = d\sigma/d\varepsilon$ (Fig. 3). At − 196 °C, θ values are $\mu_1/3$ or $\mu_2/7$; they decrease with increasing temperature and reach $\mu/20$ at room temperature. At Néel temperature, θ values show a sharp increase (Fig. 3); this increase disappears for θ/μ_2. The slip geometry suggests to look for a hardening mechanism similar to that of NaCl structure crystal [30]. Dislocations from the various slip planes intersect and become jogged or combine to form locks. Jog dragging increases the amount of point defects; dipoles and prismatic loops can be created. Slip on other planes (cross-slip) occurs to overcome obstacles or locks. This will be easier at higher temperatures and perhaps explains the drop of θ value above 400 °C (Fig. 3).

Values of $\mu/170$, $\mu/200$, $\mu/300$ and $\mu/550$ are found for MgO [22], NiO [2], NaCl [27] and LiF [29] respectively at room temperature. A difficulty remains to explain why such mechanism hardens CoO more than other compounds.

4.2 PHASE STABILITY AND PLASTIC DEFORMATION. — Two observations seem to be related to the phase transformation from CoO to Co_3O_4. First, yield stresses are constant between 0 °C and 600 °C (Fig. 3) with large unusual values which drop above 900 °C. Second, unstable yielding appeared when straining close to 1 000 °C. This unstable yielding suggests Portevin Le Chatelier effect (dynamic strain ageing); it is related to athermal plastic properties

$$(2\,000\ b^3 < V < 4\,000\ b^3)$$

but serrations are different from those usually observed [31] and plastic strength is very small. The Portevin Le Chatelier effect is observed usually for low purity materials, and our CoO crystals were very pure (§ 2.2). We have too few experiments to put forward any firmer explanation.

In order to have more information on the origin of the strength of CoO, we performed experiments at fixed oxygen pressure (air) and various temperature (Fig. 3). Crystals harden rapidly as soon as they enter the Co_3O_4 phase field i.e. below 900 °C (thermal equilibrium of the equipment is reached after one to two hours); after annealing 8 hours between 700 °C and 800 °C, the flow stress values were never larger than those measured in the 0-600 °C range (Fig. 3) using quenched specimens (§ 2.2).

We also performed experiments at fixed temperature (780 ± 25 °C) for two oxygen pressures i.e. air and flowing argon corresponding respectively to Co_3O_4 and CoO (Fig. 1). Here again, CoO hardens when it enters the Co_3O_4 field; it takes 3 h for this hardening process to be effective (Fig. 4). The crystals do not soften quickly when back in the CoO field (Fig. 4 : 17 hours from 768° in air to 756° in argon).

When CoO is placed in the Co_3O_4 field, oxidation can occur producing a very thin layer. This layer can alter the plastic behaviour by a surface effect changing dislocation mobility. Such an effect has been observed at room temperature for several materials in various media [32]. It can explain instantaneous and reversible hardening, which does not occur for CoO.

Precipitates cannot appear in the bulk of a specimen, except through oxygen pipe diffusion or vacancy annihilation :

$$3\,Co_{Co} + 4\,O_o + V_{Co} \rightarrow Co_3O_4\,.$$

The rate of precipitation depends on temperature through diffusion processes. It seems able to explain the hardening at temperatures of 700°-800 °C, but one must note that specimens, tested between 0 °C and 600 °C, should be hardened by precipitates or clusters formed during quenching and should have reached a maximum hardening. Such mechanism seems more likely than forest dislocation cutting one.

The results show that dislocation mobility is very sensitive to thermodynamic state of materials because of more or less reversible precipitation or defect clustering.

4.3 MICROHARDNESS. — Hardness anisotropy has been investigated for several compounds, using various orientation of Knoop or Vickers indentor in a given crystallographic face [33], [34]. Hardness values are seldom given for various faces; we have summarized in table II a few results for crystals known to have the { 110 } $\langle 1\bar{1}0 \rangle$ glide system. It is surprising to find that most crystals show hardness values very similar for different faces except NiO and, perhaps, MgO (Table II) which are harder in { 110 } than in { 100 } and Cu_2O which is harder in { 100 }. It has been checked that the { 110 } $\langle 1\bar{1}0 \rangle$ system is also activated when indenting { 110 } face of MgO [38], { 111 } face of NaCl [39] and { 110 } face of Cu_2O [34].

Although CoO seems very strong in compression

Table II. — *Room temperature hardness values for several compounds. Knoop hardness is anisotropic; we have given an average value.*

		H (MPa) { 100 }	{ 110 }	{ 111 }	Ref.
		—	—	—	—
Vickers	MgO	7 500 to 11 300			[33] p. 180
Vickers	NiO	4 800	7 060	6 160	[35]
Vickers	NiO	5 300			[36]
Vickers	Cu_2O		1 880		[34]
Vickers	CoO	2 970	2 800	2 750	T = 22 °C
Knoop	LiF	900 ± 30	920 ± 50	930	
Knoop	MgO	5 900 ± 1 900	6 750 ± 2 550		[33] p. 202
Knoop	MnO	2 680 ± 160	2 700 ± 180		
Knoop	Cu_2O	1 650 ± 170	1 550 ± 180		[34]

(Figs. 3 and 6), its hardness values are smaller than those of MgO, NiO (Table II).

Hardness values can be compared to other crystal properties ; this can be done if they have been measured for specimens of the same origin. The ratio H/σ is greater than 100 for NiO (Table II, Fig. 3) and 37 for CoO ; the value for CoO fits with rocksalt crystals (H/σ = 35 [33], p. 55), but it does not for NiO. The ratio value has been related to the difficulty to activate other glide systems, like { 100 } ⟨ 110 ⟩ in the rocksalt structure [37] ; the high value for NiO suggests a very high plastic anisotropy. Another kind of correlation has been made between H and θ ; it is found that H/θ is about 5 for NiO and 1 ± 0.2 for CoO, instead of expected similar values [40].

Values of H/C_{44} have been ascribed to various types of bonding : 0.1 for covalent one, 0.006 for f.c.c. metals. For ionic solid with the rocksalt structure, H/C_{44} decreases from 0.04 to 0.006 as T/T_M increases from 0.1 to 0.5 [41]. For CoO and NiO, room temperature is close to 0.14 T_M. Their chemical bonding is known to be ionic (ionicity factors ~ 0.8 to 0.85). For CoO we find

$$H/C_{44} = 0.036 \; (C_{44} = 8.32 \times 10^{10} \text{ Pa [20]})$$

and for NiO

$$H/C_{44} = 0.046 \; (C_{44} = 1.1 \times 10^{11} \text{ Pa [42]}) ;$$

these values are close to those for rocksalt crystals.

Magnetic ordering is perhaps responsible for the special properties of NiO and CoO. For CoO, a small anomaly is shown in a very narrow range of temperature for hardness values of (100) face (~ 20 %) and possibly on (110) and (111) faces (Fig. 5) ; it cannot be compared to that observed in compression tests (Fig. 3).

5. **Conclusions.** — Hardness test is widely used to correlate hardness values with numerous physical properties. NiO has higher elastic constants c_{ij} and hardness values H than CoO, but lower yield stress σ and work-hardening rate θ. Correlation between H and C_{44} seems valid for both oxides in terms of rocksalt crystals with ionic bonding.

The plastic properties of CoO depend on the thermodynamic conditions of the test ; its large strength is probably related to some precipitation. However, quenching does not give rise to increased hardness values. These contradictory observations indicate how difficult it is to have coherent results on materials tested out of thermodynamic equilibrium.

Antiferromagnetic ordering seems to influence plastic deformation of both nickel and cobalt oxides ; the role of spin ordering, cristallographic distorsion and domain walls needs to be clarified, in particular in the vicinity of the Néel temperature.

References

[1] HALES, R., *Corros. Sci.* **12** (1972) 555.

[2] DOMINGUEZ-RODRIGUEZ, A., CASTAING, J. and PHILIBERT, J., *Mater. Sci. Eng.* **27** (1977) 217.

[3] KRISHNAMACHARI, V., NOTIS, M. R., *Acta Metall.* **25** (1977) 1307.

[4] CLAUER, A. H., SELTZER, M. S., WILCOX, B. A., *J. Mater. Sci.* **6** (1971) 1379.

[5] KRISHNAMACHARI, V., JONES, J. T., *J. Am. Ceram. Soc.* **57** (1974) 506.

[6] KRISHNAMACHARI, V., *J. Mater. Sci.* **11** (1976) 1031.

[7] NEHRING, V. W., SMYTH, J. R., MCGEE, T. D., *J. Am. Ceram. Soc.* **60** (1977) 173 and 328.

[8] KRISHNAMACHARI, V., NOTIS, M. R., SHAH, D. M., *J. Mater. Sci.* **12** (1977) 666.

[9] VINJAMURI, K., NOTIS, M. R., SHAH, D. M., *Mater. Sci. Eng.* **32** (1978) 185.

[10] MUAN, A., *5th Int. Symp. Reactivity Solids*, Munich. Elsevier Pub. Co, Amsterdam (1964) 598.

[11] SREEDHARAN, O. M., CHANDRSEKHARAIAH, M. S., KARKHANAVALA, M. D., *High Temp.* **9** (1977) 109.

[12] OTT, W. R. and RANKIN, D. T., *J. Am. Ceram. Soc.* **62** (1979) 203.

[13] NOWOTNY, J., ZIOLKOWSKI, J., *Z. Anorg. Allg. Chem.* **433** (1977) 287.

[14] COLAITIS, D., FIEVET-VINCENT, F., GUÉNOT, J., FIGLARZ, M., *Mat. Res. Bull.* **6** (1971) 1211.

[15] CYR, J. P., Thèse d'état ; Institut National polytechnique de Lorraine (1976).

[16] SAURAT, M., REVCOLEVSCHI, A., *Rev. Int. Hautes Temp. Refract.* **8** (1971) 291.

[17] BRETHEAU, T., CADOZ, J., DOLIN, C., PELLISIER, B. and SPENDEL, M., *Ind. Ceram.* **694** (1976) 293.

[18] Unpublished results, Laboratoire de Physique des Matériaux.
[19] DENTSCHUCK, P. and PALMER, S. B., *Phys. Lett.* **47A** (1974) 343.
[20] ALEKSANDROV, K. S., SHABANOVA, L. A. and RESHCHIKOVA, L. M., *Sov. Phys. Solid State* **10** (1968) 1316.
[21] SUZUKI, T. and KIM, H., *J. Phys. Soc. Japan* **39** (1975) 1566.
[22] SRINIVASAN, M. and STOEBE, T. G., *J. Mater. Sci.* **9** (1974) 121.
[23] ARGON, A. S. and PADAWER, G. E., *Philos. Mag.* **25** (1972) 1073.
[24] SRINIVASAN, M. et STOEBE, T. G., *J. Mater. Sci.* **8** (1973) 1567.
[25] REMAUT, G., LAGASSE, A. and AMELINCKX, S., *Phys. Status Solidi* 7 (1964) 497.
[26] NAGAMIYA, T., SAITO, S., SHIMONURA, Y. and UCHIDA, E., *J. Phys. Soc. Japan* **20** (1965) 1285.
[27] ARGON, A. S., NIGAM, A. K. and PADAWER, G. E., *Philos. Mag.* **25** (1972).
[28] MROWEC, S. and PRZYBYLSKI, K., *Bull. Acad. Pol. Sci., Ser. Sci. Chim.* **XXV** (1977) 869.
[29] FOTEDAR, H. L. and STOEBE, T. G., *Phys. Status Solidi* (a) **31** (1975) 399.
[30] ADDA, Y., DUPOUY, J. M., PHILIBERT, J. and QUÉRÉ, Y., *Eléments de Métallurgie Physique* Tome **5,** chapitre 35 (La Documentation Francaise, Paris) 1979.
[31] DOMINGUEZ RODRIGUEZ, A. and CASTAING, J., *Scr. Metall.* **9** (1975) 551.
[32] LATANISION, R. M. and BECKHAM, K. F., *C.R.C. Crit. Rev. Solid State Sci.* **7** (1978) 317.
[33] *The Science of hardness testing and its research applications*, Edited by J. H. Westbrook and H. Conrad ; Amer. Soc. Met. 1973.
[34] AUDOUARD, A., PELLISIER, B. and CASTAING, J., *J. Phys. Lett.* **38** (1977) L-33 ; and A. Audouard, Thèse de 3e cycle, Université Paris 6.
[35] CONDE, C. F., DOMINGUEZ RODRIGUEZ, A., CONDE, A. and MARQUEZ, R., *Phys. Status Solidi* (a) **33** (1976) K 25.
[36] CABRERA CAÑO, J., DOMINGUEZ-RODRIGUEZ, A., MARQUEZ, R. and CASTAING, J., *Revue Phys. Appl.* **14** (1979) 559.
[37] GILMAN, J. J., *J. Appl. Phys.* **44** (1973) 982.
[38] PATEL, A. R. and SUTARIA, J. N., *J. Phys. D.* **4** (1971) 1586.
[39] BOYARSKAYA, Yv. S., SHUTOVA, S. S. and ZHITARU, R. P., *Phys. Status Solidi* (a) **30** (1975) K 7.
[40] GERK, A. P., *J. Mater. Sci.* **12** (1977) 735.
[41] CHIN, G. Y., WERNICK, J. H., GEBALLE, T. H., MAHAJAN, S., NAKAHARA, S., *Appl. Phys. Lett.* **33** (1978) 103.
[42] DU PLESSIS, P. V., VAN TONDER, S. J., ALBERTS, L., *J. Phys.* **4** (1971) 1983.